



Since January 2020 Elsevier has created a COVID-19 resource centre with free information in English and Mandarin on the novel coronavirus COVID-19. The COVID-19 resource centre is hosted on Elsevier Connect, the company's public news and information website.

Elsevier hereby grants permission to make all its COVID-19-related research that is available on the COVID-19 resource centre - including this research content - immediately available in PubMed Central and other publicly funded repositories, such as the WHO COVID database with rights for unrestricted research re-use and analyses in any form or by any means with acknowledgement of the original source. These permissions are granted for free by Elsevier for as long as the COVID-19 resource centre remains active.



# Post COVID-19 Head and Neck Mucormycosis: MR Imaging Spectrum and Staging

Maha Ibrahim Metwally, Mohamed Mobashir, Ahmed Hassan Sweed, Sara Mohamed Mahmoud, Aya Gamal Hassan, Kamal ElKashishy, Mohamed Eesa, Ismail Elnashar, Ashraf Elmalt, Ahmed Ibrahim Elsayed, Shaimaa Khaled Idris, Al Shaimaa Fathi Elshetry

**Objective:** To develop a systematic approach for magnetic resonance imaging (MRI) analysis, imaging spectrum, and classification system for the staging of post-COVID-19 head and neck mucormycosis.

**Method:** The study included 63 post-COVID-19 patients with pathologically proven mucormycosis who underwent head and neck MR imaging. Three independent radiologists assessed the imaging spectrum of mucormycosis, MRI characteristics of sino-nasal mucormycosis, and extra-sinus extension, and submitted a final staging using a systematic approach and a proposed categorization system. A consensus reading was considered the reference imaging standard. The kappa statistics were used to assess the categorization system's diagnostic reliability.

**Results:** The overall interreader agreement of the MR staging system was very good ( $k$ -score = 0.817). MR imaging spectrum involved localized sino-nasal mucormycosis ( $n = 7$  patients, 11.1%), sino-nasal mucormycosis with maxillo-facial soft tissue extension ( $n = 28$  patients, 44.5%), sino-nasal mucormycosis with maxillo-facial bony extension ( $n = 7$  patients, 11.1%), sino-naso-orbital mucormycosis ( $n = 13$  patients, 20.6%), and sino-nasal mucormycosis with cranium or intracranial extension ( $n = 8$  patients, 12.7%). Extra-sinus extension to the orbit and brain did not have significant association with involvement of the posterior ethmoid/sphenoid sinuses and maxillo-facial regions ( $p > 0.05$ ). MRI-based staging involved four stages: stage 1 ( $n = 7$ , 11.1%); stage 2 ( $n = 35$ , 55.6%), and stage 3 ( $n = 13$ , 20.6%), and stage 4 ( $n = 8$ , 12.7%). Involvement of the bone and MR-based staging were significant predictors of patients' mortality  $p = 0.012$  and  $0.033$ , respectively.

**Conclusion:** This study used a diagnostic-reliable staging method to define the imaging spectrum of post-COVID-19 head and neck mucormycosis and identify risk variables for extra-sinus extension.

**Key Words:** Mucormycosis; COVID-19; Magnetic resonance imaging; risk factors.

© 2021 The Association of University Radiologists. Published by Elsevier Inc. All rights reserved.

## INTRODUCTION

COVID-19 has predisposed to secondary infections, especially in critically ill patients with a tenfold increase in fungal infections (1). Mucormycosis, a rare fungal infection, is the most fulminant form of Zygomycosis caused by Mucorales species of the phylum Zygomycota (2).

### Acad Radiol 2022; 29:674–684

From the Lecturer of Radio-diagnosis, Faculty of Human Medicine, Zagazig University, Egypt (M.I.M., A.S.F.E.); Professor of Otorhinolaryngology-Head and Neck Surgery, Faculty of Human Medicine, Zagazig University, Egypt (M.M., I.E., A.E., A.I.E.); Lecturer of Otorhinolaryngology-Head and Neck Surgery, Faculty of Human Medicine, Zagazig University, Egypt (A.H.S., M.E.); Assistant lecturer of Radio-diagnosis, Faculty of Human Medicine, Zagazig University, Egypt (S.M.M., A.G.H., S.K.I.); Professor of Pathology, Faculty of Human Medicine, Zagazig University, Egypt (K.E.). Received November 14, 2021; revised December 8, 2021; accepted December 8, 2021. **Address correspondence to:** M.I.M. e-mail: [aleenys009@gmail.com](mailto:aleenys009@gmail.com)

© 2021 The Association of University Radiologists. Published by Elsevier Inc. All rights reserved.  
<https://doi.org/10.1016/j.acra.2021.12.007>

Literature has established a link between COVID-19 infection, corticosteroid use, immunocompromised states such as diabetes mellitus (DM), and mucormycosis (3–7).

Head and neck Mucormycosis starts with sporangiospores inhalation, direct extension to the paranasal sinuses, and hyphae angioinvasion in immunocompromised hosts, resulting in subsequent necrotizing vasculitis, fungal thrombi, and tissue infarctions (8,9). The fungus spreads through occlusion of vascular vessels or direct invasion through the superior orbital fissure, cribriform plate, whereas vascular invasion occurs through ophthalmic vessels. Intracranial involvement is also caused by carotid artery or perineural invasion (10,11). Mucormycosis involvement in the head and neck is divided into four categories: isolated nasal, sino-nasal, rhino-orbital, and rhino-orbital-cerebral mucormycosis (12).

Mucormycosis diagnosis depends on the clinical features, pathological criteria, and imaging findings that assess the

extent of involvement (13). Early detection and treatment of mucormycosis can save lives, since a 1 week delay in treatment raises mortality from 35% to 66%. (14). Since surgical debridement of devitalized tissue is crucial for the optimal therapy of mucormycosis (15), radiologists should be aware of the anatomical sites that must be evaluated in order to determine the extent of mucormycosis infection and be familiar with the different imaging patterns.

As an extension of literature discussing COVID-19 associated mucormycosis (1,16,17), this study aims to define the imaging spectrum and distinct imaging features of head and neck Mucormycosis after COVID-19 infection, as well as propose an imaging-based classification system based on mucormycosis regional involvement and test its reliability.

**MATERIALS AND METHODS**

**Ethical Considerations**

The study was permitted by our ethics committee (IRB approval no. 7014). Written informed consent was acquired from all patients in our study. The study was compliant with the ethical principles of the declaration of Helsinki. This

manuscript was reported in adherence with the Strengthening the Reporting of Observational Studies in Epidemiology.

**Study Design and Population**

From June 2021 to September 2021, a cross section study was conducted. All of the patients had a history of COVID-19 infection (which was confirmed by laboratory, clinical, and radiological means) and were referred to our radiology department in Zagazig University for magnetic resonance imaging (MRI) at the request of their otorhinolaryngologists. Inclusion criteria included: (i) confirmed infection with COVID-19 within the previous 3 months (ii) clinically suspected mucormycosis patients (e.g., black necrotic turbinate, blood-tinged nasal discharge with ipsilateral facial pain, peri-orbital or facial swelling, skin induration and discoloration, ptosis of the eyelid, and ophthalmoplegia). Exclusion criteria were (i) patients refused surgical interference ( $n = 1$ ), (ii) absent pathological evaluation of the surgical specimens ( $n = 1$ ), (iii) patients who previously had sino-nasal fungus infection or underwent prior endoscopic sinus surgery ( $n = 3$ ), (iv) patients with pathologically proven mixed fungal infection or bacterial sinusitis ( $n = 6$ ). Our final sample included sixty-three patients.

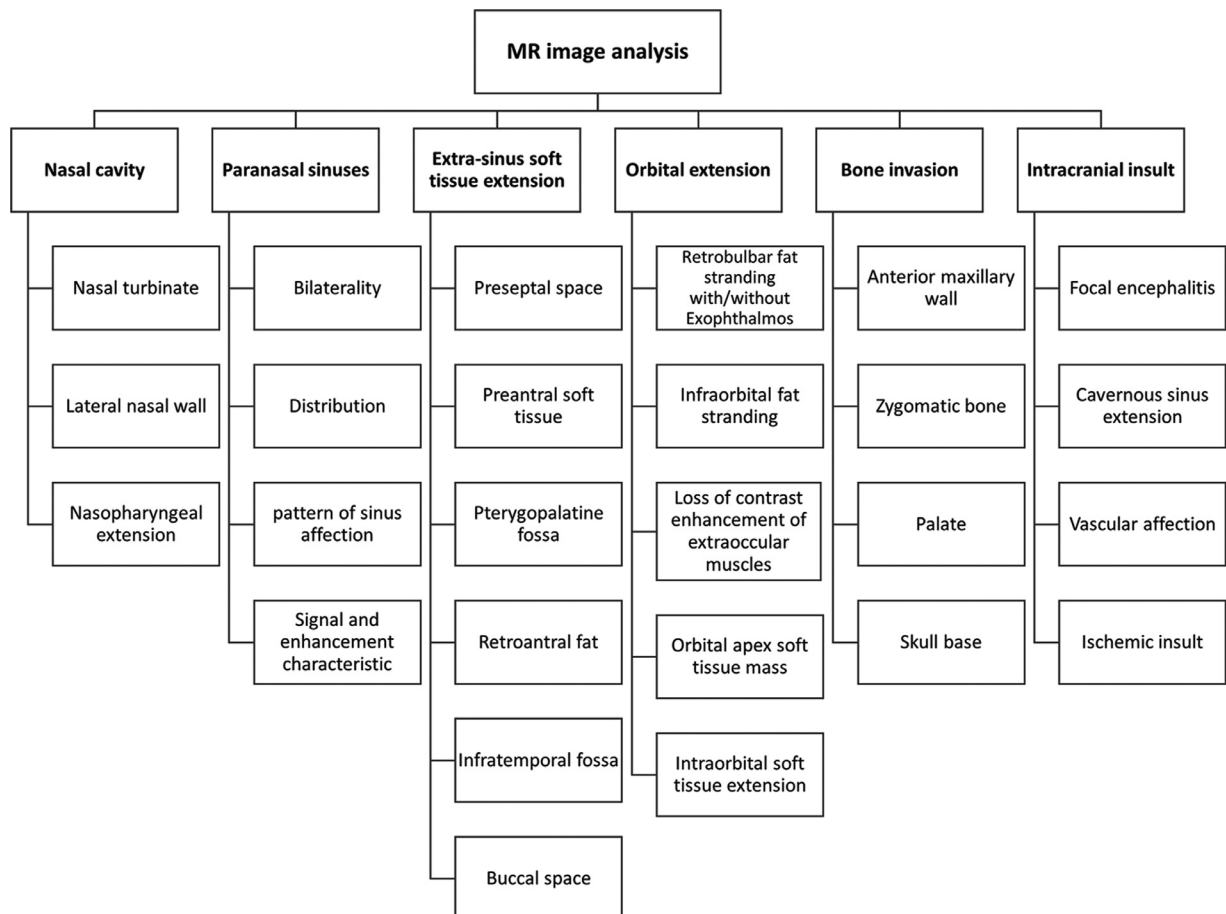


**Figure 1.** Systematic approach for MRI analysis in head and neck mucormycosis.

**TABLE 1. Demographic and clinical data of patients**

Characteristic	Value
Total No. of patients	63
Age, (years), mean $\pm$ SD (range)	58.3 $\pm$ 8.47 (40-75)
Sex	
Male	22 (34.9)
Female	41 (65.1)
History of corticosteroid intake	52 (82.5)
Mean period of corticosteroid use, (weeks), mean (range)	2.6 (1-8)
Comorbidities	
DM	51
Hypertension	26
Chronic liver disease	7
Heart failure	5
Chronic obstructive pulmonary disease	4
Asthma	2
Thyrotoxicosis	1
Multiple myeloma	1
Time interval between COVID-19 and mucormycosis, (weeks), mean (range)	3.12 (1-8)
Clinical presentation*	
Ptosis, ophthalmoplegia and proptosis	43
Facial and eye swelling	39
Facial palsy	7
Loss of vision	4
Blood tinged nasal discharge	35
Headache	47
Patients outcome	
Survived	52 (82.5)
Died	11 (17.5)

\*Each patient may experience multiple symptoms.

Note. Unless stated otherwise, data are number of patients and data in parentheses are percentages.

SD, Standard deviation.

### MR Image Acquisition

All patients underwent paranasal MR examination using a 1.5-Tesla MRI system (Achieva-class IIa, Philips Medical Systems) with a standard head coil. The paranasal MRI protocol included axial T1-weighted (T1WI) turbo spin echo (TSE) images (echo time (TE): 10 millisecond (ms), repetition time (TR): 550 ms, field of view (FOV): 230 $\times$ 199, matrix: 232 $\times$ 179, gap: 0.4mm) with and without fat saturation (fat-sat); axial T2-weighted (T2WI) TSE images (TE: 90 ms, TR: 2960 ms, FOV: 230 $\times$ 198, matrix: 288 $\times$ 210, gap: 0.4mm); axial T2W spectral presaturation with inversion recovery high resolution (SPIR-HR) images (TE: 90 ms, TR: 2960 ms, FOV: 230 $\times$ 198, matrix: 288 $\times$ 210, gap: 0.4mm), coronal T2W-SPIR images (TE: 80 ms, TR: 2993 ms, FOV: 240 $\times$ 188, matrix: 292 $\times$ 198, gap: 0.4mm), sagittal, coronal, and axial post-contrast T1W with and without fat-sat images (TE: 21 m, TR: 573 ms, FOV: 252 $\times$ 226, matrix: 280 $\times$ 197, gap: 0.4mm). Additional brain MRI sequences were performed in all patients included axial T1WI and

**TABLE 2. MR imaging characteristics of sinonasal mucormycosis**

MR imaging characteristics	Number of patients (percentage)
Pattern of sinus affection	
Sinus mucosal thickening	25 (39.7)
Complete sinus opacification	10 (15.9)
Combined patterns	28 (44.4)
T1WI Signal	
Hypointense	63 (100)
T2WI signal	
Hyperintense	23 (36.5)
Heterogeneous (peripheral high signal + central low signal)	40 (63.5)
Sinus enhancement	
Absent	35 (55.6)
Present	28 (44.4)
Homogeneously enhanced sinus mucosa	5 (7.9)
Heterogeneously enhanced sinus (Bubbly appearance)	23 (36.5)
Black turbinate sign	
Absent	33 (52.4)
Present	30 (47.6)

T2WI, axial fluid attenuation inversion recovery (FLAIR), axial diffusion-weighted (DW) image at b-value 0 and 1000, and axial, sagittal, and coronal post-contrast T1W-TSE.

### MR Images Analysis

Figure 1 depicts a systematic approach to MR imaging analysis in mucormycosis of the head and neck. All MR images were analysed separately by each radiologist who was blinded to the patients' clinical data, then a final reading was reached in consensus, according to this prescribed methodical manner.

### MR imaging-based staging system

We categorized mucormycosis regional extension in the head and neck into 4 stages; stage 1: involvement of the nose and paranasal sinuses (PNS) with no extra-sinus extension, subcategorized into 1a and 1b with and without involvement of posterior ethmoid air cells and sphenoid sinus, respectively, stage 2: extra-sinus maxillo-facial extension subcategorized into 2a soft tissue extension, 2b maxillo-facial bone involvement, stage 3: maxillofacial and orbital extension, subcategorized into 3a extraconal extension and 3b intraconal soft tissue extension, and stage 4: cranium and intracranial extension subcategorized into 4a skull base or anterior cranial fossa extension, 4b cavernous sinus involvement, 4c focal cerebritis, and 4d local vasculitis or direct vascular invasion with and/or without cerebral infarction. According to the total regional expansion, patients were assigned the highest stage.

**TABLE 3. Analysis of mucormycosis extra-sinus extension and related MRI findings**

Site of extra-sinus extension	Number of patients (percentage)	MRI findings
No extra-sinus extension	7 (11.1)	—
Maxilla-facial soft-tissue		
Pterygopalatine fossa	49 (77.8)	Infiltration of the involved soft-tissue spaces with fat stranding manifested mainly on T2 fat-sat sequence
Preantral soft tissue	47 (74.6)	
Retroantral fat	34 (54)	
Infra-temporal fossa	25 (39.7)	
Preseptal space	29 (46)	
Buccal space	3 (4.8)	
Maxillo-facial bones		
Anterior maxillary and zygomatic bone	1 (15.9)	Destruction of the involved facial bones, with low T1W and T2W SI
Maxillary process of palatine bone	6 (9.5)	
Orbit		
Intrabital intra-conal fat	10 (15.9)	Stranding of the retrobulbar fat on T2 fat-sat sequence
Intrabital intra-conal soft tissue extension	4 (6.3)	Enhanced intraconal soft tissue
Extra-ocular muscles	4 (6.3)	Thickening and decreased enhancement of extra-ocular muscles
Infraorbital fat	5 (8)	Stranding of infraorbital fat on T2 fat sat sequence
Skull base	2 (3.2)	Alteration of the bone marrow signal at the involved clivus and pterygoid bone with low T1W and T2W SI
Intracranial		
Cavernous sinus	1(1.6)	Enhanced cavernous sinus
Cavernous ICA ectasia	1(1.6)	Ectasia of the cavernous portion of ICA
Focal cerebritis	1 (1.6)	Focal nonvascular territorial based-distribution T2 and FLAIR hyperintense, non-enhanced area with restricted diffusion
Cerebral infarction	3 (4.8)	Cortical and subcortical T2 and FLAIR hyperintense non-enhanced area with restricted diffusion following the vascular territory or in the watershed area

T1W, T1-weighted; T2W, T2-weighted; SI, signal intensity; ICA, internal carotid artery; FLAIR, fluid attenuation inversion and recovery.

### Surgical Management

Surgical debridement was performed with an average lag time of 3.2 days from admission and intervention; during this time, all patients received systemic antifungal medication and underwent MR examination. According to MRI findings, the endoscopic procedure was recommended. During the operation, all necrotic tissues were removed until healthy vascular tissue was visible. Enucleation was performed in cases of intraconal soft tissue extension.

### Reference Standard

Pathological analysis of surgical specimens validated the diagnosis of mucormycosis. The presence or absence of histological criteria for mucormycosis previously identified in the literature, such as the presence of broad, aseptate, or pauci-septate hyphae with wide-angle branching in the afflicted tissue with and/or without tissue invasion, were interpreted on specimens (18).

### Statistical Analysis

The Shapiro-Wilk test was used to check and confirm the normal distribution of the data. When applicable, the data of the recruited

patients were expressed as mean, standard deviation (SD), and range, or number and percentage. The association between involvement of the posterior ethmoid and sphenoid sinuses, maxillo-facial spaces, and extra-sinus extension to the orbits and brain was determined using Pearson's correlation. Patients' outcomes (independent variable) were dichotomized (died and survived) and multiple logistic regression analysis was used to assess the relationship between multiple predictor variables (demographic, clinical, and imaging characteristics, and staging system) and patients' outcomes in the early post-operative period. Weighted kappa scores (k-score) were employed to assess the diagnostic reliability of the proposed staging system. K-score of less than 0.20 represented poor agreement; 0.21–0.40 represented fair agreement; 0.41–0.60 represented moderate agreement; 0.61–0.80 represented good agreement; and 0.81–1 represented very good agreement. Statistical analyses were accomplished using "SPSS version 23". The *P*-value was statistically significant if less than 0.05.

## RESULTS

### Patient Demographic and Clinical Characteristics

A total of 63 consecutive post-COVID-19 patients (22 males and 41 females) were enrolled in the study with a mean age

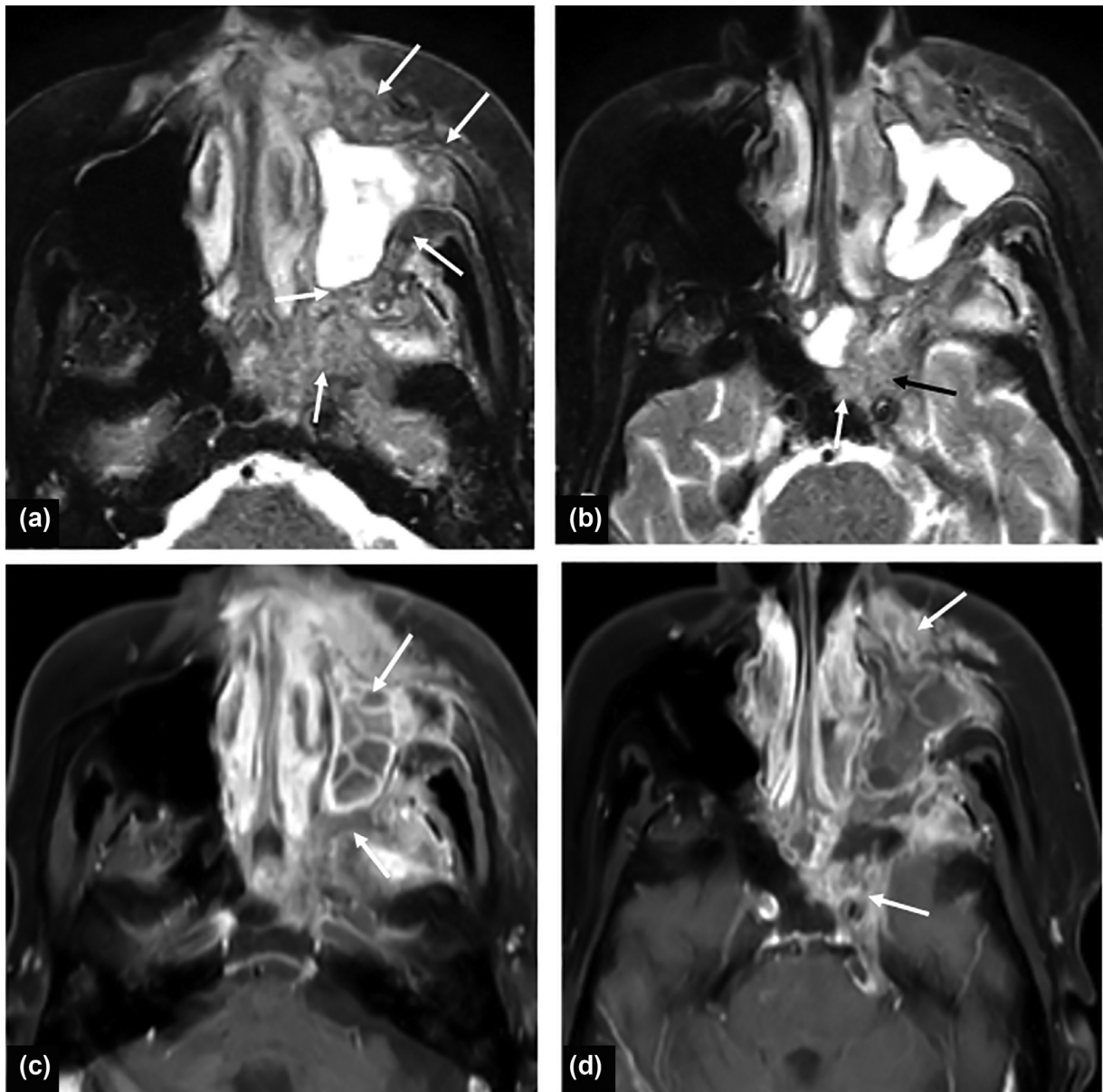


**Figure 2.** A 63-year-old diabetic and hypertensive female patient who experienced left facial swelling, ptosis, and chemosis 3 weeks following COVID-19 infection, and received corticosteroid for 2 weeks. (A) and (B) axial T2W-SPIR images reveal complete opacification of the left maxillary sinus with homogeneous high signal intensity, and precisely demarcates the extension of the T2 high signal intensity anteriorly into the preantral region and zygomatic bone, and posteriorly into the left pterygopalatine fossa, retroantral fat, infratemporal fossa, left hemi-clivus, and cavernous sinus (arrows), (C) and (D) axial post-contrast T1W-fat-sat images showing “soap bubble sign” of the left maxillary sinus (arrows in C) with enhanced tissue at the left preantral, infratemporal, and cavernous sinus regions (arrows in D). Stage 4b (sinonasal mucormycosis with cranial extension).

$\pm$  SD of  $58.3 \pm 8.47$  years (age range, 40-75). The mean time interval between COVID-19 and mucormycosis infection was three weeks (range, 1-8 weeks). The total number of deaths during the early postoperative period (up to day-8 post-operative) was 11 (17.5%) patients (Table 1).

#### MR imaging spectrum

The imaging spectrum of mucormycosis was localized sino-nasal mucormycosis ( $n = 7$  patients, 11.1%); sino-nasal mucormycosis with maxillo-facial soft tissue extension

( $n = 28$  patients, 44.5 %); sino-nasal mucormycosis with maxillo-facial bony extension ( $n = 7$  patients, 11.1%); sino-naso-orbital mucormycosis ( $n = 13$  patients, 20.6%); sino-nasal mucormycosis with cranium or intracranial extension ( $n = 8$  patients, 12.7%).

#### MR imaging characteristics of sino-nasal mucormycosis

Table 2 shows the pattern of sinus involvement, signal intensity, and enhancement characteristics on MR imaging. The most commonly involved paranasal sinus (PNS) was the

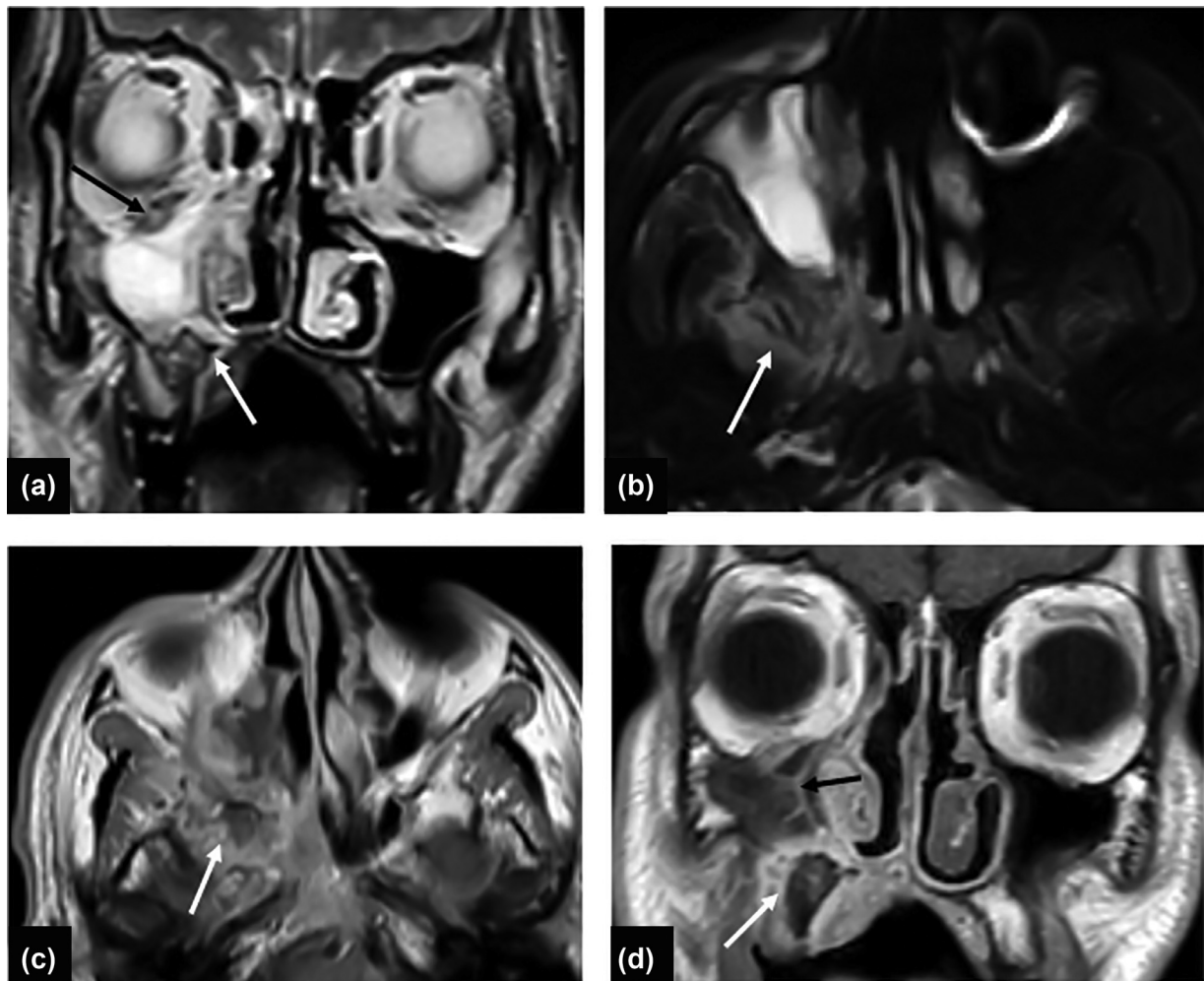


**Figure 3.** A 53-year-old diabetic male patient presented with right facial palsy 1 month following COVID-19 infection, and received corticosteroid for 2 weeks (A) coronal T2W-TSE image reveals total opacification of the right maxillary and ethmoid air cells with high T2 signal intensity and hypointense septa, and destruction of the right superior alveolar margin and palate (white arrow), black arrow points to infiltration of infraorbital fat (B) axial T2W-SPIR demarcates the extension of infection into pterygopalatine and infratemporal fossa (arrow) (C) and (D) axial and coronal post contrast T1W-TSE images showing extension of infection into the right infratemporal fossa and palate, black arrow in D points to soap bubble appearance of the right maxillary sinus. Stage 3a (sinonasal mucormycosis with maxillo-facial soft tissue, bone extension, and intraorbital extraconal fat infiltration).

maxillary sinus ( $n = 63$ , 100%). 45 of 63 (71.4%) patients had multiple sinus affection ( $\geq 3$  sinuses). Unilateral sinus involvement was more common ( $n = 35/63$ , 55.6%) than bilateral sinus affection. In contrast-enhanced T1WI, 90% of the completely opacified maxillary sinuses displayed heterogeneous enhancement manifested with multiple enhanced septa on a background of non-enhanced sinus, giving a “soap bubble appearance” sign.

#### MRI analysis of extra-sinus extension

The sites and patterns of extra-sinus extension are summarized in Table 3. The most frequent site of extra-sinus extension was the pterygopalatine fossa ( $n = 49$ , 77.8%).

Figures 2-6 show demonstrative cases

#### Diagnostic reliability and Assignment of the proposed MR staging system

The overall interreader agreement of the MR staging system was very good ( $\kappa = 0.81$ ). Table 4 displays the staging of mucormycosis according to regional involvement in the head and neck. The prevalence of mucormycosis in stages 1, 2, 3, and 4 mucormycosis was 11.1, 55.6, 20.6, and 12.7%, respectively.

#### Assessment of risk factors of extra-sinus extension

Based on the results of Pearson’s correlation, there was no statistically significant association between the involvement of the posterior ethmoid and sphenoid sinuses and extra-sinus

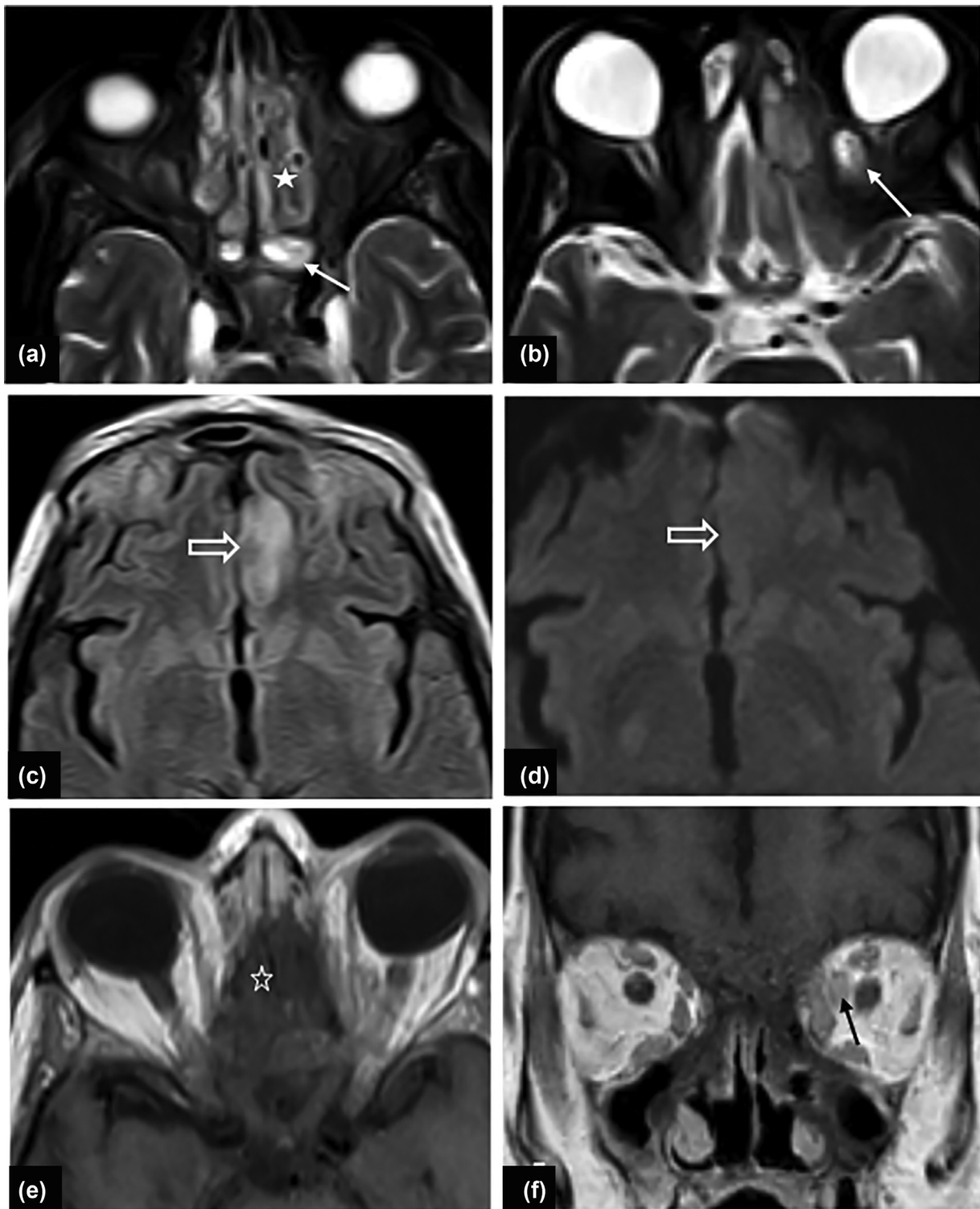


**Figure 4.** A 50-year-old diabetic and hypertensive female patient presented with left side ptosis, chemosis, limited left eye mobility, and confusion 14 days following COVID-19 infection, received corticosteroid for 12 days (A and B) axial T2W-SPIR reveal opacification of the both ethmoid air cells and sphenoid sinuses with heterogeneous T2 signal intensity, left intraconal soft tissue extension is noted (arrow in B) (C) axial FLAIR shows left inferior frontal cortical and subcortical high signal intensity compatible to area of facilitated diffusion on DWI at b-value 1000 (D). (E and F) axial and coronal post-contrast T1WI show non-enhancing ethmoid sinuses with enhanced intraconal soft tissue extension (black arrow in F). Stage 4c (rhino-cerebro-orbital mucormycosis).

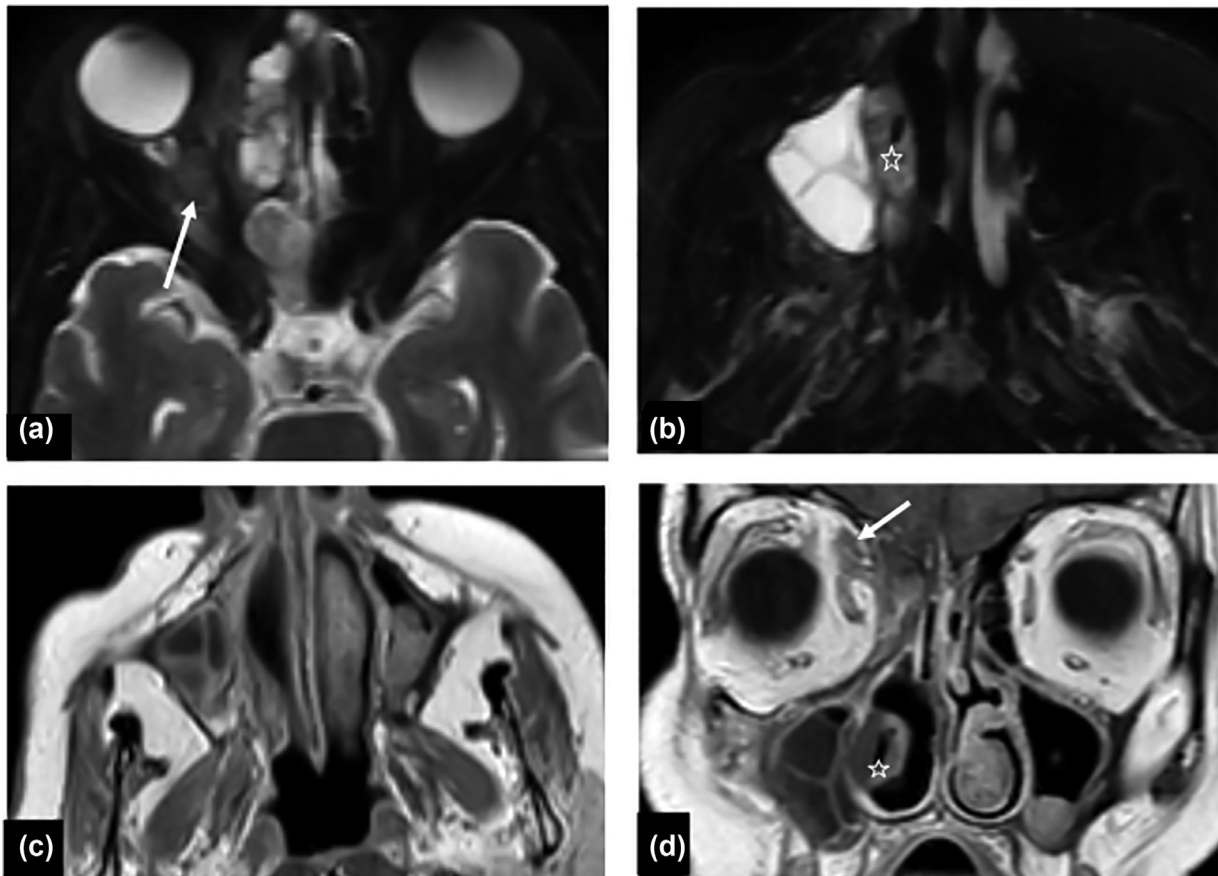


**Figure 5.** A 70-year-old diabetic and hypertensive female patient presented with right eye swelling, chemosis and facial pain 21 days following COVID-19 infection, no history of corticosteroid usage. (A) and (B) axial T2W-SPIR image reveals complete opacification of the right ethmoid air cells with heterogeneous signal intensity, and right maxillary sinus with multiple hypointense septa on top of hyperintense signal, white arrow in (A) points to right intraorbital soft tissue extension white star in (B) points to necrotic right turbinate, (C) and (D) axial and coronal post-contrast T1W-TSE images showing soap bubble sign of right maxillary sinus, necrotic non-enhanced right turbinate “black turbinate sign” (white star in D), white arrow in (D) points to the intraorbital intraconal enhanced soft tissue. Stage 3b (sino-naso-orbital mucormycosis).

extension to the orbit and brain ( $p = 0.567$  and  $0.796$ , respectively). Similarly, there was no significant association between the involvement of the maxillo-facial spaces by mucormycosis and extra-sinus extension to the orbit and brain ( $p = 0.877$  and  $0.672$ , respectively).

#### Predictors of patients' outcomes

Multiple variables were evaluated to determine their predictive value for the patients' outcomes. Based on multiple logistic regression analysis, MRI-based stage and bone invasion indicated a significant correlation with patients' mortality,  $p \leq 0.001$ . The mortality rate was higher in stage 4 (7 patients) and stage 2b (4 patients). Other variables including age, gender, co-morbidity, corticosteroid administration, and imaging spectrum had insignificant association with patients' mortality,  $p = 0.623, 0.499, 0.412, 0.236,$  and  $0.251$ , respectively.

#### Surgical Outcome

All patients underwent endoscopic debridement of devitalized fungal infected tissue through modified Denker approach. In addition, six patients underwent inferior maxillectomy, while another one underwent facial resection. Two patients with non-serviceable eyes were treated by orbital exenteration. In patients with partial visual loss, orbital debridement was performed. Operative findings demonstrated a pink or pale, firm, gritty mass with little vascularity infiltrating the underlying tissue.

#### Fungal Smear and Histopathological Results

All of the specimens examined contained hyalinized necrotic tissue with aggregates of inflammatory cells and numerous mucormycosis fungal hyphae. These hyphae infiltrated the tissue and/or bone. There was no evidence of atypia or malignancy.

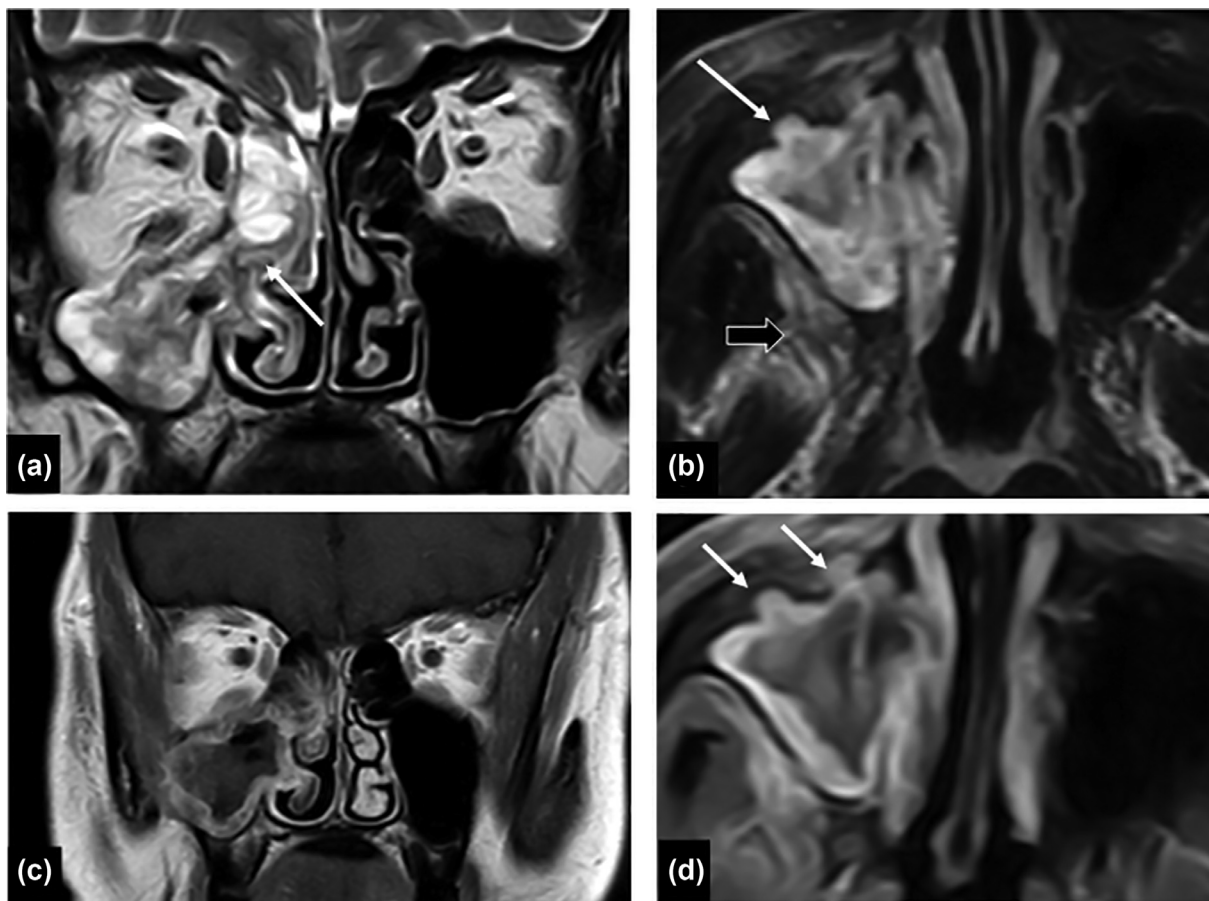


**Figure 6.** A 56-year-old hypertensive female patient presented with right eye swelling, ptosis, chemosis and facial pain 21 days following COVID-19 infection, received corticosteroid for 10 days. (A) coronal T2W-TSE image shows complete opacification of the right maxillary sinus and ethmoid air cells by heterogeneous signal with loss of the normal signal intensity of the right nasal turbinate, white arrow points to destroyed lateral nasal wall (B) axial T2W-SPIR image reveals destroyed right anterior maxillary wall marked by white arrow, thick black arrow points to abnormal high signal of the retroantral fat and infratemporal fossa (C) coronal post-contrast T1W-TSE image shows enhanced maxillary sinus mucosa with non-enhanced center, and right black turbinate sign (D) axial post contrast T1W- fat-sat image shows erosion of the anterior maxillary wall marked by arrows. Stage 2b (sino-nasal mucormycosis with maxillo-facial bone and soft tissue extension).

## DISCUSSION

The current study demonstrated a systematic approach for the analysis of MR imaging in head and neck mucormycosis patients, allowing for a thorough assessment of mucormycosis regional involvement and potential sites of extension in the head and neck region. Also, it revealed different imaging spectra of the disease including, localized sino-nasal mucormycosis, sino-nasal mucormycosis with maxillo-facial soft tissue extension, sino-nasal mucormycosis with maxillo-facial bone extension, sino-naso-orbital mucormycosis, sino-nasal mucormycosis with cranium or intracranial extension. We identified staging system of mucormycosis regional involvement in the head and neck and demonstrated its diagnostic reliability. This classification should improve communication between radiologists and otorhinolaryngologists and standardize the reporting of mucormycosis cases.

In general, head and neck mucormycosis is the most frequent variant of mucormycosis infection that accounts for

50% of the patients (19). It is more common in diabetics and immunosuppressed patients (20,21). In the current study, we focused on assessing head and neck mucormycosis in post-COVID-19 patients. Superinfection and coinfection with COVID-19 are still being investigated to determine whether they are caused by the virus or its management. (1). High-dose corticosteroids, which are commonly used to treat COVID-19, especially in the presence of DM may result in hyperglycemia and acidosis which increases the risk of mucormycosis by eliciting phagocytes dysfunction (3). Several research investigations have attempted to establish a relationship between DM and mucormycosis (8,22). According to two meta-analyses, DM was the most common predisposing factor for mucormycosis, accounting for 40%-64% of cases (23,24), and a global rate of 17%-88% (25). In our study, diabetes mellitus was reported in 81% of mucormycosis cases and history of corticosteroid usage was positive in 82.5%.

The black turbinate sign, (non-enhancing, hypointense turbinate), sinus opacification, air-fluid level, variable intensity

**TABLE 4. MR imaging-based classification of mucormycosis staging**

Staging	Site of involvement	Number of patients (percentage)
Stage 1	Involvement of the nose and PNS with no extra-sinus extension	7 (11.1)
Stage 1a	Involvement of the nose and PNS except posterior ethmoidal and sphenoidal sinuses.	2
Stage 1b	Involvement of all PNS including posterior ethmoidal and sphenoidal sinuses but no extra-sinus extension.	5
Stage 2	Extra-sinus maxillo-facial extension	35 (55.6)
Stage 2a	Maxillo-facial soft tissue extension, including soft tissue spaces (e.g., preantral, buccal, preseptal, retro antral spaces, pterygopalatine fossa, infratemporal fossa) and/or orbit.	28
Stage 2b	Maxillo-facial bone involvement	7
Stage 3	Extra-sinus maxillofacial and orbital extension	13 (20.6)
Stage 3a	Extraconal extension	9
Stage 3b	Intraconal soft tissue extension	4
Stage 4	Cranium and intracranial extension	8 (12.7)
Stage 4a	Skull base bones or anterior cranial fossa extension	2
Stage 4b	cavernous sinus involvement	1
Stage 4c	Focal cerebritis	1
Stage 4d	Cerebral vascular insult.	4

PNS, paranasal sinus.

within the sinuses on T1- and T2-weighted images (predominant hypointense on T2), obliteration of the nasopharyngeal planes, preantral fat infiltration, loss of contrast enhancement of the sino-nasal mucosa and extraocular muscles, inflammatory changes in the extraocular muscles and fat, and cerebral leptomeningeal enhancement were all previously documented MR findings of acute fulminant invasive fungal sinusitis (AFIFS) (26,27). In the current study, we concluded that mucormycosis imaging features in post COVID-19 patients did not vary from those previously documented in AFIFS. Except for cerebral leptomeningeal enhancement, all of the previously described MRI features of mucormycosis were detected in varying degrees in the current study.

Son et al. (28) reported that 93% (13 cases) of rhino-cerebral-orbital mucormycosis (RCOM) patients had sinus mucosal thickening and air-fluid level with no cases with full sinus opacification. On contrary, in the current study, complete sinus opacification was documented in 60.3% (38/63) of the cases. An interesting finding was observed that 90% of cases with complete maxillary sinus opacification showed heterogeneous post-contrast enhancement in the form of enhanced septa on the background of non-enhanced sinus giving a “soap bubble appearance sign”. This sign may be explained by the necrotizing nature of fungal infection and it was previously documented in 68.8%–70% of cases with chronic invasive fungal sinusitis and named as septal enhancement with a sensitivity of 39.4%–42.4% and a specificity of 87.2%–91.5% (29).

The extra-sinus fat infiltration is caused either by vascular congestion-related edema or fungal infiltration, and it can even happen before bone osteolysis occurs because the fungus spreads primarily through perivascular channels (30,31). Therefore, in our study, patients with maxillo-facial extension were assigned distinct subcategories in the proposed

staging system depending on the absence (stage 2a) and presence of bone invasion (stage 2b). Retroantral fat pad inflammation, osseous erosion, and orbital extension, according to Gorovoy et al. (30) were specific but late and less prevalent characteristics of AFIFS. However, we reported the involvement of the retroantral fat, facial bones, and orbit in 54% (34/63), 11.1% (7/63), and 20.6% (13/63) of our patients, respectively. Furthermore, contrary to Howells et al. study (26), maxillo-facial bone infiltration was not always a late finding in our mucormycosis cases, and it can even occur without significant extrasinus soft tissue involvement. This could be attributed to the behavior of invasive fungal extension via trans vascular route rather than direct extension. Similarly, direct vascular invasion or embolic seeding causes fungal spread to the orbit and cerebral tissues (30). In addition, Mathur et al. (32) found an association between posterior ethmoid and sphenoid sinus affection and an increased risk of intracranial extension. Nonetheless, there was no statistically significant association between infiltration of the posterior ethmoid and sphenoid sinuses, as well as the maxillo-facial spaces, and extra-sinus extension to the orbit and brain in our study. Finally, we concluded that the reported MRI-based mucormycosis staging had a significant relationship with patient mortality, suggesting that it could be a useful predictor of patient outcome, and recommend further evaluation of its prognostic value in other literature.

We acknowledge that our research has some limitations. To begin with, our study had a small sample size, which was due to our inclusion and exclusion criteria. Second, we relied on the patients' short-term follow-up since we chose to explore early death rates among mucormycosis patients rather than the frequently measured late (e.g., 90 day) mortality rates. Finally, we did not take into account the pulmonary

condition of post-covid-19 patients, which could affect the death rate at different stages.

## CONCLUSIONS

In conclusion, in post-COVID-19 patients, this study established a systematic approach for appropriate MRI assessment of mucormycosis infection in the head and neck region, as well as distinct imaging spectra of head and neck mucormycosis. Also, an imaging-based diagnostic-reliable staging system of mucormycosis was assigned, which could enhance the accuracy of MR reporting and consequently better outcome.

## REFERENCES

- Maini A, Tomar G, Khanna D, et al. Sino-orbital mucormycosis in a COVID-19 patient: A case report. *Intern J of Surg Case Reports* 2021; 1(82):105957.
- Sugar AM. *Mucormycosis Clin. Infect. Dis* 1992; 14:S126–S129.
- Corzo-León DE, Chora-Hernández LD, Rodríguez-Zulueta AP, et al. Diabetes mellitus as the major risk factor for mucormycosis in Mexico: epidemiology, diagnosis, and outcomes of reported cases. *Med Mycol* 2018; 56:29–43.
- Bonaventura A, Montecucco F. Steroid-induced hyperglycemia: An underdiagnosed problem or clinical inertia? A narrative review. *Diabetes Res Clin Pract* 2018; 139:203–220.
- Spellberg B, Edwards J, Ibrahim A. Novel perspectives on mucormycosis: pathophysiology, presentation, and management. *Clin Microbiol Rev* 2005; 18:556–569.
- Tan L, Wang Q, Zhang D, et al. Lymphopenia predicts disease severity of COVID-19: a descriptive and predictive study. *Signal Transduct Target Ther* 2020; 5:1–3.
- Li J, Wang X, Chen J, et al. COVID-19 infection may cause ketosis and ketoacidosis. *Diabetes Obes Metab* 2020; 22:1935–1941.
- Liu M, Spellberg B, Phan QT, et al. The endothelial cell receptor GRP78 is required for mucormycosis pathogenesis in diabetic mice. *J. Clin. Invest* 2010; 120:1914–1924.
- Serris A, Danion F, Lantermier F. Disease entities in mucormycosis. *J of Fungi* 2019; 5:23.
- Bawankar P, Lahane S, Pathak P, et al. Central retinal artery occlusion as the presenting manifestation of invasive rhino-orbital-cerebral mucormycosis Taiwan. *J. Ophthalmol* 2020; 10:62–65.
- Parsi K, Itgampalli RK, Vittal R, et al. Perineural spread of rhino-orbito-cerebral mucormycosis caused by *Apophysomyces elegans*. *Ann. Indian Acad. Neurol* 2013; 16:414.
- Safi M, Ang MJ, Patel P, et al. Rhino-orbital-cerebral mucormycosis (ROCM), and associated cerebritis treated with adjuvant retrobulbar amphotericin B. *Am. J. Ophthalmol. Case Rep* 2020; 19:100771.
- Deutsch PG, Whittaker J, Prasad S. Invasive and non-invasive fungal rhinosinusitis—a review and update of the evidence. *Medicina* 2019; 55:1–14.
- Werthman-Ehrenreich A. Mucormycosis with orbital compartment syndrome in a patient with COVID-19. *Am. J. Emerg. Med* 2021; 42(264):e5–264.e8.
- Tissot F, Agrawal S, Pagano L, et al. ECIL-6 guidelines for the treatment of invasive candidiasis, aspergillosis and mucormycosis in leukemia and hematopoietic stem cell transplant patients. *Haematologica* 2017; 102:433–444.
- Mehta S, Pandey A. Rhino-orbital mucormycosis associated with COVID-19. *Cureus* 2020; 12(9):e10726.10.7759.
- Therakathu J, Prabhu S, Irodi A, et al. Imaging features of rhinocerebral mucormycosis: A study of 43 patients. *The Egyptian J of Radiol and Nucl Med* 2018; 49:447–452.
- De Pauw B, Walsh TJ, Donnelly JP, et al. Revised definitions of invasive fungal disease from the European Organization for Research and Treatment of Cancer/Invasive Fungal Infections Cooperative Group and the National Institute of Allergy and Infectious Diseases Mycoses Study Group (EORTC/MSG) Consensus Group. *Clin Infect Dis* 2008; 46:1813–1821.
- Dan M. Mucormycosis of the head and neck. *Current infectious disease reports* 2011; 13:123–131.
- Spellberg B, Edwards J, Jr Ibrahim A. Novel perspectives on mucormycosis: pathophysiology, presentation, and management. *Clin Microbiol Rev* 2005; 18:556–569.
- Roden MM, Zaoutis TE, Buchanan WL, et al. Epidemiology and outcome of zygomycosis: a review of 929 reported cases. *Clin Infect Dis* 2005; 41:634–653.
- Ibrahim AS, Spellberg B, Walsh TJ, et al. Pathogenesis of mucormycosis. *Clin. Infect. Dis* 2012; 54:S16–S22.
- Jeong W, Keighley C, Wolfe R, et al. The epidemiology and clinical manifestations of mucormycosis: a systematic review and meta-analysis of case reports. *Clinical Microbiology and Infection* 2019; 25:26–34.
- Vaughan C, Bartolo A, Vallabh N, et al. A meta-analysis of survival factors in rhino-orbital-cerebral mucormycosis—has anything changed in the past 20 years? *Clin. Otolaryngol* 2018; 43:1454–1464.
- Prakash H, Chakrabarti A. Global epidemiology of mucormycosis. *J of Fungi* 2019; 5:26.
- Howells RC, Ramadan HH. Usefulness of computed tomography and magnetic resonance in fulminant invasive fungal rhinosinusitis. *Am J Rhinol* 2001; 15:255–261.
- Safder S, Carpenter JS, Roberts TD, et al. The “Black Turbinate” sign: an early MR imaging finding of nasal mucormycosis. *AJNR Am J Neuroradiol* 2010; 31:771–774.
- Son JH, Lim HB, Lee SH, et al. Early differential diagnosis of rhino-orbito-cerebral mucormycosis and bacterial orbital cellulitis: based on computed tomography findings. *PLoS ONE* 2016; 11:e0160897.
- Li Z, Wang X, Jiang H, et al. Chronic invasive fungal rhinosinusitis vs sinonasal squamous cell carcinoma: the differentiating value of MRI. *European radiology* 2020; 30:4466–4474.
- Gorovoy IR, Kazanjian M, Kersten RC, et al. Fungal rhinosinusitis and imaging modalities. *Saudi J of Ophthalmol* 2012; 26:419–426.
- Gamba JL, Woodruff WW, Djang WT, et al. Craniofacial mucormycosis: assessment with CT. *Radiology* 1986; 160:207–212.
- Mathur S, Karimi A, Mafee MF. Acute optic nerve infarction demonstrated by diffusion-weighted imaging in a case of rhinocerebral mucormycosis. *AJNR Am J Neuroradiol* 2007; 28:489–490.